JOURNAL OF SOLID STATE CHEMISTRY 114, 95–101 (1995)

An Investigation of Insulating $La_4BaCu_5O_{12}$ Obtained by the Reduction of Metallic $La_4BaCu_5O_{13.1}$[1]

N. Rangavittal, G. N. Subbanna, T. N. Guru Row, and C. N. R. Rao[2]

Solid State and Structural Chemistry Unit, Indian Institute of Science, Bangalore 560 012, India

Received November 2, 1993; in revised form April 4, 1994; accepted April 4, 1994

The structure of insulating $La_4BaCu_5O_{12}$ obtained by the reduction of metallic $La_4BaCu_5O_{13.1}$ has been studied by using electron microscopy and high-resolution X-ray diffraction data. While $La_4BaCu_5O_{13.1}$ ($P4/m$) has a tetragonal structure with the supercell $a_c\sqrt{5} \times a_c\sqrt{5} \times a_c$, the reduced phase, $La_4BaCu_5O_{12}$, is monoclinic ($P2/m$) with the supercell $a_c\sqrt{5} \times a_c \times a_c\sqrt{5}$. $La_4BaCu_5O_{12}$ consists of CuO_5 square pyramids and CuO_4 square planar units, instead of CuO_6 octahedra and CuO_5 square pyramids as in $La_4BaCu_5O_{13.1}$. Electron microscopic examination reveals the presence of twinning in some of the crystals of $La_4BaCu_5O_{12}$.

INTRODUCTION

$La_4BaCu_5O_{13+\delta}$ is an interesting oxygen-deficient perovskite composed of corner sharing CuO_5 square pyramids and CuO_6 octahedra containing Cu(II) and Cu(III) ions (1). It has a tetragonal structure ($P4/m$) with a supercell of type $a_c\sqrt{5} \times a_c\sqrt{5} \times a_c$. It is possible to partially substitute La with other rare earth ions (2). Oxygen stoichiometry in $La_4BaCu_5O_{13+\delta}$ can be varied to induce a metal–insulator transition (3). Defect perovskite phases with $\delta = -0.5$ and -1.0 have been identified by Davies and Katzan (4) and more recently by Kato *et al.* (5).

Davies and Katzan (4) reported a monoclinic structure for $La_4BaCu_5O_{12.5}$ ($\delta = -0.5$) based on X-ray diffraction. Kato *et al.* (5) confirmed the monoclinic structure for this composition and reported that it had the supercell $a_c\sqrt{10} \times a_c\sqrt{10} \times a_c$ based on electron diffraction. Davies and Katzan also reported $La_4BaCu_5O_{12}$ ($\delta = -1.0$) to be monoclinic, but the detailed structure was not investigated; no supercell has been reported for this composition. Since these ordered defect compositions are formed by the reduction of $La_4BaCu_5O_{13+\delta}$ containing Cu in two oxidation states with different types of oxygen coordination, we have investigated the detailed structure and the associated Cu coordination in $La_4BaCu_5O_{12}$ obtained by the removal of one oxygen from the parent tetragonal cuprate $La_4BaCu_5O_{13.1}$.

[1] Contribution No. 965 from the Solid State & Structural Chemistry Unit.

[2] To whom correspondence should be addressed.

EXPERIMENTAL

$La_4BaCu_5O_{13+\delta}$ was prepared starting with an appropriate mixture of $BaCO_3$, La_2O_3, and CuO. The mixture was decarbonated at 1170 K, followed by heating at 1270 K for 48 hr (1). The X-ray powder pattern of the sample so obtained was identical to that reported in the literature. The oxygen content of the cuprate was determined by heating the sample in a Cahn TG 131 balance under a stream of 15% H_2 + 85% Ar mixture. Around 1170 K the sample was fully reduced to a mixture of barium and lanthanum oxides with Cu metal. The initial oxygen content was calculated from the weight loss during the reduction. Oxygen-deficient $La_4BaCu_5O_{12}$ was prepared by heating the parent cuprate to approximately 670 K under a 15% H_2 + 85% Ar atmosphere, followed by quenching to room temperature.

Electron microscopic studies were carried out in a JEOL 200 CX electron microscope fitted with a top-entry double tilt stage. Samples for microscope observation were prepared by grinding the powders finely and depositing them on carbon-coated grids. Electron diffraction patterns and bright-field images of many crystals were recorded. Through-focus high-resolution images were also recorded on selected thin crystals in the magnification range $3–5 \times 10^5$. $La_4BaCu_5O_{13.1}$ and $La_4BaCu_5O_{12}$ were also subjected to Rietveld profile analysis by using data obtained with a STOE X-ray powder diffractometer. Diffraction data were recorded at 0.02 intervals every 4 sec from 8°–80° in 2θ using a linear PSD. The indexing and the profile refinements on these samples were carried out using the STADI/P package (6).

RESULTS AND DISCUSSION

Thermogravimetric analysis of $La_4BaCu_5O_{13+\delta}$ showed δ to be 0.1, independent of heat treatment, up to 1270 K. The structure was tetragonal $P4/m$ and most of the crys-

0022-4596/95 $6.00

tals gave electron diffraction patterns showing the presence of the supercell $a_c\sqrt{5} \times a_c\sqrt{5} \times a_c$ (Fig. 1). some isolated crystals gave an electron diffraction pattern corresponding to $a_c\sqrt{10} \times a_c\sqrt{10} \times a_c$ due to the ordering of the excess oxygen ($\delta = 0.1$). In Fig. 2, we show a high-resolution image of the $La_4BaCu_5O_{13+\delta}$. The inset of this figure shows a magnified region revealing the positions of the Ba ions. The structural projection along (001) is also shown in the inset. A detailed X-ray profile analysis by the Rietveld procedure showed the presence of Cu in both the octahedral and square-pyramidal coordinations, in agreement with the values reported by Michel *et al.* (1); the results are shown in Table 1, where the refined atomic coordinates are listed. The *R* factors obtained are entirely satisfactory and we show the observed, calculated, and difference X-ray diffraction patterns in Fig. 3 to illustrate the quality of agreement.

$La_4BaCu_5O_{12}$ prepared by the reduction of $La_4BaCu_5O_{13.1}$ around 670 K under a stream of 15% H_2 + 85% Ar gave electron diffraction patterns corresponding to a monoclinic structure with a supercell of $a_c\sqrt{5} \times a_c \times a_c\sqrt{5}$ (Fig. 4). The material was insulating unlike the parent cuprate. High resolution X-ray diffraction patterns of $La_4BaCu_5O_{12}$ could be indexed on the basis of the same monoclinic supercell. X-ray diffraction profiles of this phase were sharp (Fig. 5) and were subjected to Rietveld analysis.

$La_4BaCu_5O_{13+\delta}$ has a tetragonal space group $P4/m$ and the reduced phase therefore has the least symmetric reduced subgroup, $P2/m$. Davies and Katzan (4) have also obtained the same unit cell parameters and space group for this phase. If the structure has to follow the symmetry-directed pathway from $P4/m$ to $P2/m$, each coordinate of all the atoms in the structure has to undergo the tetragonal-to-monoclinic distortion. Considering each

TABLE 1
Atomic Parameters of $La_4BaCu_5O_{13.1}$ ($P4/m$) with a = 8.665(6) Å, c = 3.867(3) Å

Atom	Site	x	y	z	Occupancy	U (Å²)
La1	4*k*	0.1263(1)	0.2764(1)	0.5	1.0	0.0085(2)
Ba1	1*d*	0.5	0.5	0.5	1.0	0.0185(6)
Cu1	1*a*	0.0	0.0	0.0	1.0	0.0073(1)
Cu2	4*j*	0.4161(2)	0.1711(1)	0.0	1.0	0.0244(6)
O1	1*b*	0.0	0.0	0.5	1.0	0.03[a]
O2	2*e*	0.0	0.5	0.0	0.10	0.03
O3	4*j*	0.2689(1)	0.3924(1)	0.0	1.0	0.03
O4	4*j*	0.224(2)	0.0693(1)	0.0	1.0	0.03
O5	4*k*	0.4272(1)	0.1503(1)	0.5	1.0	0.03

Note. $R_{(P)}$ = 0.046, $R_{(W,P)}$ = 0.060, $R_{(I,hkl)}$ = 0.090.
[a] Temperature factors on oxygen were fixed.

atom in Table 1, the symmetry-directed pathway can be viewed as follows. Atom La(1) located at x, y, $\frac{1}{2}$ (4*k* site) can only go to x, $\frac{1}{2}$, z (2*n* site) in $P2/m$. The other two La atoms can therefore be generated by retention of the now pseudo-fourfold relationship as $-z$, $\frac{1}{2}$, x (2*n* site). Atoms Cu(2), O(3), and O(4) which were at the 4*j* site thus generate two sets of 2*m* site atoms, while O(5) generates two sets of 2*n* site atoms. La(1) thus takes O(5) along from the 4*k* site to the 2*n* sites, and Cu(2) takes O(3) and O(4) along from the 4*j* sites to the 2*m* sites. Ba(1) and Cu(1) remain at the same coordinates, leaving O(1) and O(2) without any symmetry counterpart. As a consequence, O(1) leaves the lattice. From the neutron diffraction results (1) on $La_4BaCu_5O_{13+\delta}$, it is to be noted that O(1) has the highest temperature factor in the lattice. The removal of O(1) also correlates with the shortening of the *c* axis. This also reduces the average copper valence from 2.44 to 2.0 resulting in a distortion of the basal CuO_4

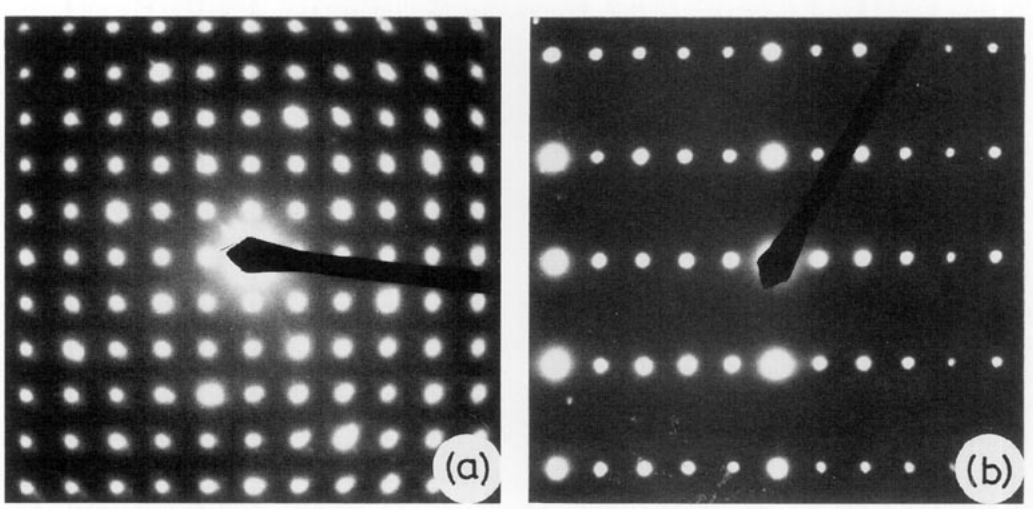

FIG. 1. Electron diffraction patterns of $La_4BaCu_5O_{13.1}$ showing the $a_c\sqrt{5} \times a_c\sqrt{5} \times a_c$ cell (a) along (001) and (b) along (010).

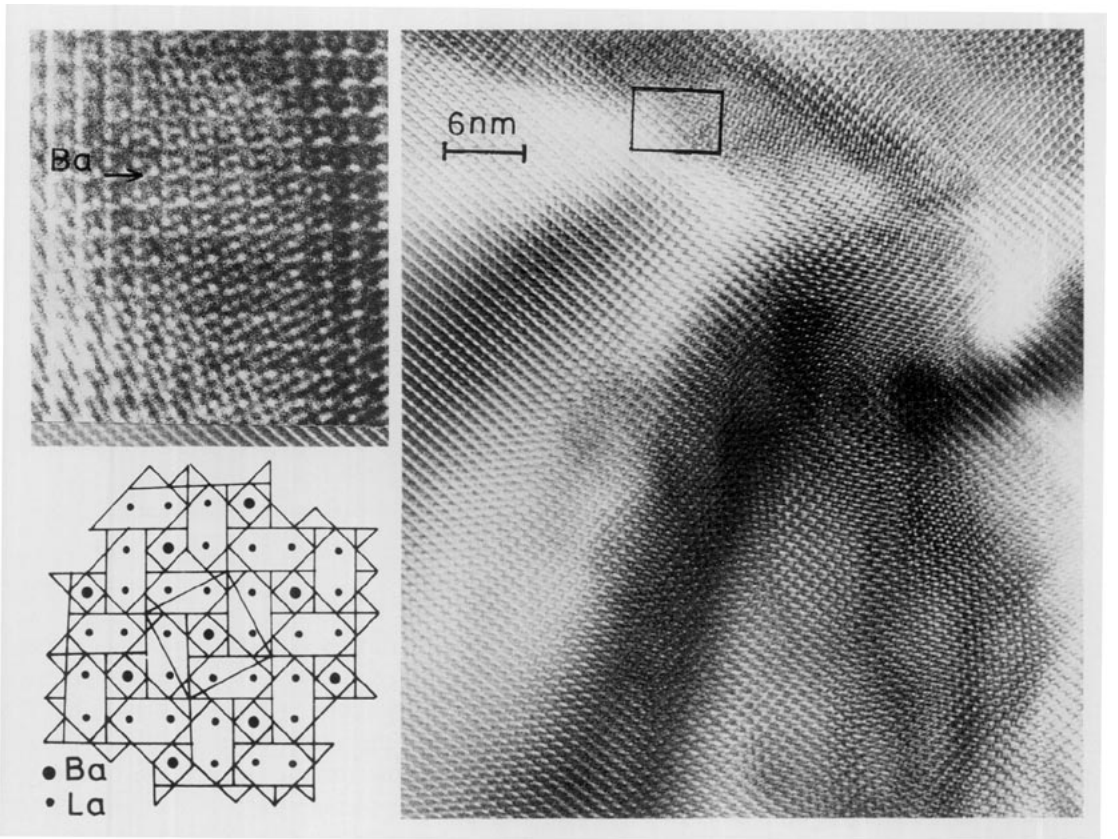

FIG. 2. High-resolution lattice image of $La_4BaCu_5O_{13.1}$ showing the positions of Ba along (001). Structural projections are shown in the inset.

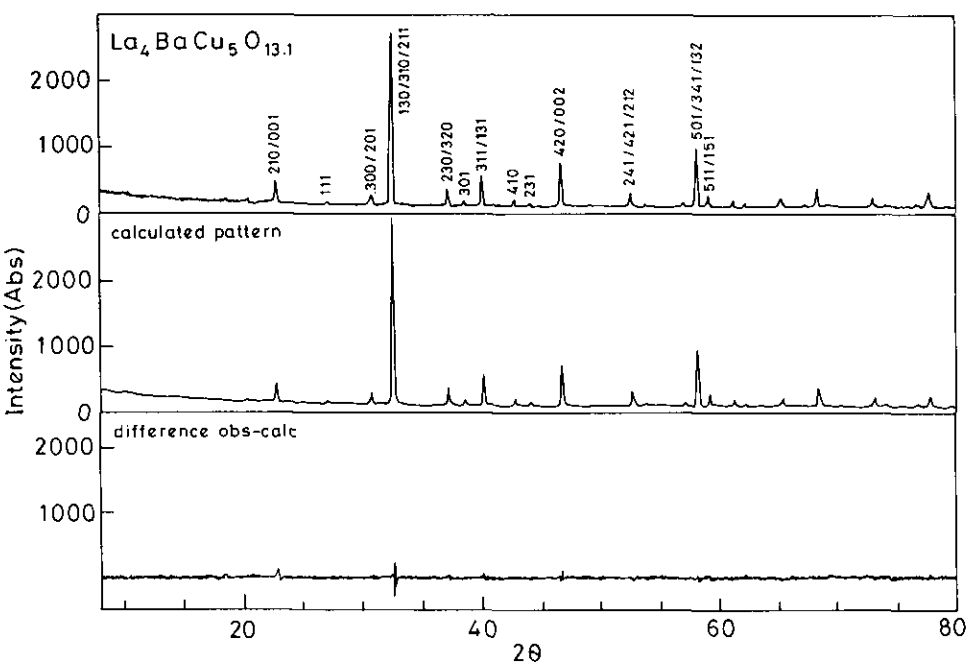

FIG. 3. Observed, calculated, and difference X-ray diffraction patterns of $La_4BaCu_5O_{13.1}$.

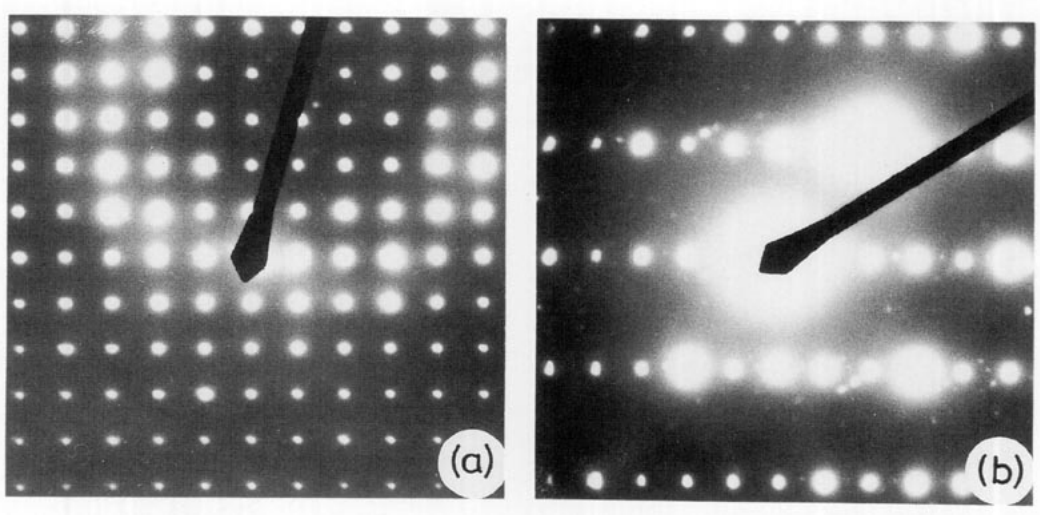

FIG. 4. Electron diffraction patterns of $La_4BaCu_5O_{12}$ showing the $a_c\sqrt{5} \times a_c \times a_c\sqrt{5}$ cell (a) along (010) and (b) along (001).

plane. Consequently, the a and b axes degenerate, causing the appearance of 201, -102, and 010 as separate lines in the X-ray diffraction pattern (Fig. 5) of the reduced phase.

Davies and Katzan (4) suggested the removal and rearrangement of oxygen ions. Of the two oxygen ions removed from the copper octahedra in the parent phase, one evolves from the lattice and the second occupies the vacant site along the a-axis. The neutron diffraction study of Michel *et al.* (1) clearly demonstrates that the vacant site is partially occupied by O(2) in the parent phase and that the Cu–O(2) distances are rather short (1.656(4) Å). Kato *et al.* (5) have pointed out that without direct experimental evidence, it is difficult to elucidate the site for the removal of oxygen. We believe that in order to allow for the occupation of the vacant site by oxygen, the tetragonal-to-monoclinic distortion is not large enough to avoid Cu–O short contacts. The positions of the heavy atoms were refined first. The positional parameters of the symmetry-related oxygens were then tied together and refined with the positional parameters of the associated copper atoms. Once the positional pa-

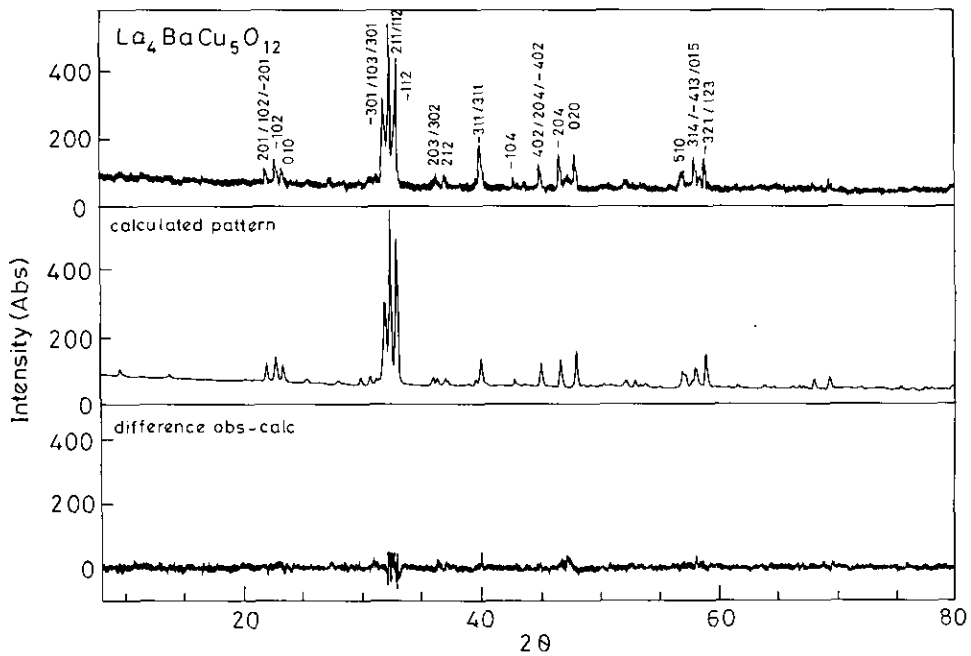

FIG. 5. Observed, calculated, and difference X-ray diffraction patterns of $La_4BaCu_5O_{12}$.

TABLE 2
Atomic Parameters of $La_4BaCu_5O_{12}$ ($P2/m$) with a = 8.901(2) Å, b = 3.771(2) Å, c = 8.691(2) Å, β = 88.60(2)°

Atom	Site	x	y	z	Occupancy	U (Å²)
La1	2*n*	0.1090(3)	0.5	0.2895(4)	1.0	0.0393(87)
La2	2*n*	−0.2638(3)	0.5	0.1286(4)	1.0	0.0393(87)
Ba1	1*h*	0.5	0.5	0.5	1.0	0.0371(14)
Cu1	1*a*	0.0	0.0	0.0	1.0	0.0236(24)
Cu2	2*m*	0.4255(7)	0.0	0.1669(8)	1.0	0.0447(21)
Cu3	2*m*	−0.1899(7)	0.0	0.4378(9)	1.0	0.0447(21)
O1	2*m*	0.2870(16)	0.0	0.3800(34)	1.0	0.03[a]
O2	2*m*	−0.3810(21)	0.0	0.2510(17)	1.0	0.03
O3	2*m*	0.2130(25)	0.0	0.0770(27)	1.0	0.03
O4	2*m*	−0.0810(24)	0.0	0.2220(30)	1.0	0.03
O5	2*n*	0.3950(23)	0.5	0.1510(19)	1.0	0.03
O6	2*n*	−0.1410(17)	0.5	0.4090(23)	1.0	0.03

Note. $R_{(P)}$ = 0.0702, $R_{(W,P)}$ = 0.0909, $R_{(I,hkl)}$ = 0.1785.
[a] Temperature factors on oxygen fixed.

rameters of all the atoms were refined to convergence, the temperature factors of the heavy atoms were released from the initial value of U = 0.04 Å².

The structural parameters of $La_4BaCu_5O_{12}$ along with the reliability factors are presented in the Table 2. The calculated and difference profiles are shown in Fig. 5 to illustrate the goodness of the fit. Removal of the O(1) apical oxygen present in the $[CuO_6]$ octahedra of $La_4BaCu_5O_{13.1}$ accounts for the loss of one oxygen per unit cell in the formation of $La_4BaCu_5O_{12}$. The $[CuO_6]$ octahedra are thus converted to $[CuO_2]$ square planes along the a–b plane. $La_4BaCu_5O_{12}$ has Cu in the square-pyramidal and square-planar coordinations instead of the square-pyramidal and octahedral coordinations as in $La_4BaCu_5O_{13.1}$, as shown in Fig. 6. The structure still retains three-dimensionality due to the linking of the $[CuO_5]$ square pyramids

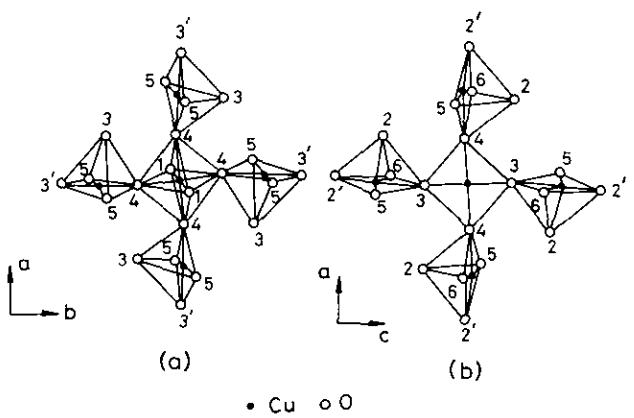

FIG. 6. (a) Cu present in octahedral coordination edge-linked to square pyramids in $La_4BaCu_5O_{13.1}$ and (b) Cu in square-planar edge-linked to square pyramids in $La_4BaCu_5O_{12}$.

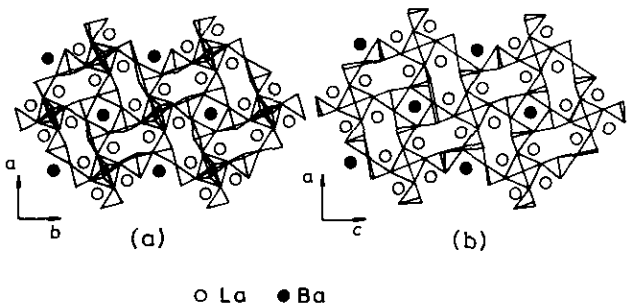

FIG. 7. Projections of (a) $La_4BaCu_5O_{13.1}$ and (b) $La_4BaCu_5O_{12}$ structures viewed along the shortest axis.

along the c axis. In Fig. 7, we show the projections of $La_4BaCu_5O_{13.1}$ and $La_4BaCu_5O_{12}$ along the shortest axis. The oxygen content per unit cell based on the copper coordination would be as follows:

$La_4BaCu_5O_{13}$: $[CuO_6]3 \times 1 = 3$,
$[CuO_{2.5}]2.5 \times 4 = 10$ {3 + 10 = 13}

$La_4BaCu_5O_{12}$: $[CuO_2]2 \times 1 = 2$,
$[CuO_{2.5}]2.5 \times 4 = 10$ {2 + 10 = 12}.

In Table 3, we compare the important bond distances in $La_4BaCu_5O_{13.1}$ and $La_4BaCu_5O_{12}$. We see the expected changes in the Cu–O distances because the square planar coordination of Cu is in the reduced phase. The Cu–O apical distance in square pyramids is about 2.37 Å in $La_4BaCu_5O_{12}$ compared to 2.30 Å in $La_4BaCu_5O_{13.1}$. The in-plane Cu–O in $La_4BaCu_5O_{13.1}$ ranges from 1.88 to 2.03 Å, whereas it is in the range 1.89–2.09 Å in $La_4BaCu_5O_{12}$.

TABLE 3
Bond Lengths (Å) in $La_4BaCu_5O_{13.1}$ and $La_4BaCu_5O_{12}$

$La_4BaCu_5O_{13.1}$	$La_4BaCu_5O_{12}$
Cu (octahedral)	Cu (square planar)
Cu(1)–O(1) → 1.935(4) × 2	Cu(1)–O(3) → 2.046(22) × 2
–O(4) → 2.032(8) × 4	–O(4) → 2.044(29) × 2
Cu (square pyramidal)	Cu (square pyramidal)
Cu(2)–O(3) → 2.303(8) × 1	Cu(3)–O(2) → 2.376(19) × 1
–O(4) → 1.884(8) × 1	–O(2′) → 1.892(10) × 1
–O(3′) → 1.863(8) × 1	–O(4) → 2.088(25) × 1
–O(5) → 1.946(4) × 2	–O(5) → 1.914(10) × 1
	–O(6) → 1.950(23) × 1
Ba–O(3) → 2.937(7) × 8	Ba–O(1) → 2.826(17) × 8
–O(5) → 3.095(8) × 4	–O(5) → 3.244(18) × 4
La–O(1) → 2.633(1) × 1	La–O(1) → 2.655(15) × 2
–O(3) → 2.506(6) × 2	–O(3) → 2.782(17) × 2
–O(4) → 2.771(7) × 2	–O(4) → 2.630(16) × 2
–O(4′) → 2.612(7) × 2	–O(5) → 2.813(17) × 2
–O(5) → 2.729(9) × 2	
–O(6) → 2.826(9) × 1	–O(5′) → 2.691(18) × 2

This increase in Cu–O distances is consistent with the reduction of Cu^{3+} to Cu^{2+}. We recall that the average oxidation state of Cu in $La_4BaCu_5O_{13.1}$ is +2.44, while it is +2 in $La_4BaCu_5O_{12}$. Some of the La–O distances in $La_4BaCu_5O_{12}$ are longer due to the increase in the *a* and *b* axes. Although the oxygen positions obtained from X-ray diffraction studies may not be exact, it seems quite certain that the basic structural features would be correct, especially with respect to the change in the Cu coordination upon reduction of $La_4BaCu_5O_{13.1}$.

The presence of copper in different coordinations, octahedral and square-pyramidal in $La_4BaCu_5O_{13+\delta}$ and square-planar and square-pyramidal in $La_4BaCu_5O_{12}$, prompts us to compare the structural parameters in these cuprates with those in cuprate superconductors (7, 8). La_2CuO_4 consist of $[CuO_6]$ octahedra with the basal Cu–O distance of 1.89 Å and an apical Cu–O distance of about 2.41 Å (9). The shorter apical Cu–O distance of 1.935 Å in the octahedra of $La_4BaCu_5O_{13+\delta}$ is probably due to the presence of Cu^{3+} in the octahedra. The displacement of two oxygens from the apex of the octahedra leads to $[CuO_4]$ square planes perpendicular to the *c* axis with a Cu–O distance of 1.90 Å, as in the case of Nd_2CuO_4 (10). Nd_2CuO_4 derivatives (11) crystallize in the T′ and T* structures. $Nd_{2-x}Ce_xCuO_4$ ($x = 0.15$) crystallizing in the T′ structure has $[CuO_4]$ square planes with a Cu–O distance of 1.973 Å, whereas $(Nd, Ce, Sr)_2CuO_4$ crystallizes in the T* structure with Cu in square-pyramidal coordination. The apical Cu–O distance of 2.22 Å and the in-plane distance of 1.936 Å in the T* structure are close to the distances found in the CuO_5 square pyramids of $La_4BaCu_5O_{13+\delta}$ and $La_4BaCu_5O_{12}$, which are also comparable to the square-pyramidal bond lengths in $YBa_2Cu_3O_7$ (2.295 and 1.92 Å). As expected, the Cu–O distance of 2.04 Å in the square-planar units of $La_4BaCu_5O_{12}$ is slightly larger than that in the $[CuO_4]$ units (1.84–1.94 Å) of $YBa_2Cu_3O_7$ and $YBa_2Cu_4O_8$ containing Cu^{3+} ions (10, 12). $YBa_2Cu_3O_7$ loses oxygen (13, 14) to form $YBa_2Cu_3O_6$ with square-pyramidal and linear coordinations. The apical Cu–O distance of 2.46 Å and the in-plane Cu–O distance of 1.94 Å in the $[CuO_5]$ units of $YBa_2Cu_3O_6$ are comparable to the distances in the $[CuO_5]$ square pyramids of $La_4BaCu_5O_{12}$.

Thallium cuprates with two or more Cu layers have Cu in square-pyramidal coordination, as, for example, in $Tl_2Ba_2CaCu_2O_8$ (15). The $[CuO_5]$ square pyramids here have a Cu–O in-plane distance of 1.92 Å and a large apical distance of 2.69 Å, rendering the square pyramids more like the square-planar units. In the 1222 thallium cuprates, Cu is in square-pyramidal coordination with a large apical Cu–O distance of 2.60 Å (16, 17), a value larger than those in $La_4BaCu_5O_{13+\delta}$ and $La_4BaCu_5O_{12}$, but the in-plane Cu–O distances are comparable. The in-plane Cu–O distances in these two cuprates are also similar to those in the 1223 Hg cuprates (18). Doping in the Ca site of $CaCuO_2$ by Sr stabilizes the infinite layer structure with a Cu–O distance of 1.93 Å (19). $La_4BaCu_5O_{12}$ also has $[CuO_4]$ square planes arranged in parallel, but with a larger in-plane distance of 2.04 Å. However, $La_2Cu_2O_5$, as reported recently by Cava *et al.* (20), consists of ribbons of La_2CuO_4 sandwiched between Cu–O planes of low dimensionality, with the Cu–O distances in the 1.97–2.10 Å range, comparable to the distances in $La_4BaCu_5O_{12}$.

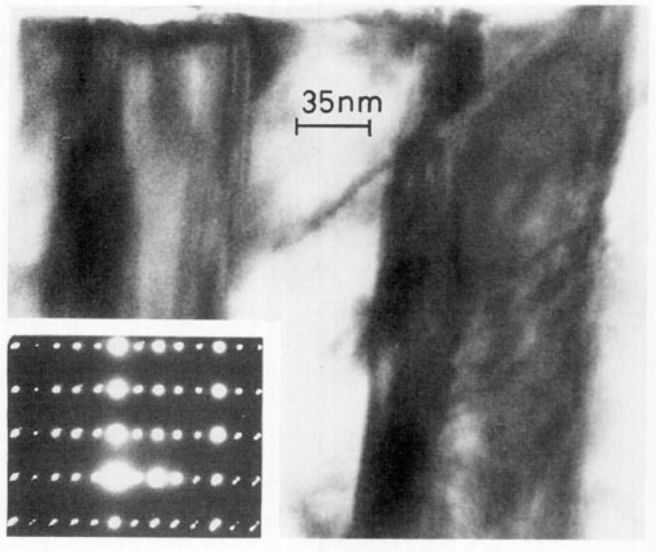

FIG. 8. Bright-field image of $\delta = -1.0$ phase showing twinning. Electron diffraction pattern from the twinned region is shown in the inset.

Electron microscopic examination of $La_4BaCu_5O_{12}$ reveals the presence of twinning in some of the crystals. Such twinning is not present in $La_4BaCu_5O_{13.1}$. A bright-field image of one such twinned grain in $La_4BaCu_5O_{12}$ is shown in Fig. 8. The selected area electron diffraction pattern in the inset clearly shows the spot splitting along *c** corresponding to twinning. Such twinned lamellae were also observed by Davies and Katzan in $LaBaCu_5O_{11.75}$.

REFERENCES

1. C. Michel, L. Er Rakho, M. Herview, J. Pannetier, and B. Raveau, *J. Solid State Chem.* **68,** 143 (1987).
2. R. Vijayaraghavan, R. A. Mohan Ram, and C. N. R. Rao, *J. Solid State Chem.* **78,** 316 (1988).
3. R. Vijayaraghavan, R. A. Mohan Ram, P. Ganguly, and C. N. R. Rao, *Mater. Res. Bull.* **23,** 719 (1988).
4. P. K. Davies and C. M. Katzan, *J. Solid State Chem.* **88,** 368 (1990).
5. M. Kato, N. Kojima, K. Yoshimura, Y. Ueda, N. Nakayama, K. Kosuge, Z. Hiroi, and Y. Bando, *J. Solid State Chem.* **103,** 253 (1993).
6. H. M. Rietveld, *J. Appl. Crystallogr.* **2,** 65 (1969).

7. C. N. R. Rao and B. Raveau, *Acc. Chem. Res.* **22,** 106 (1989).
8. C. N. R. Rao (Ed.), "Chemistry of High-temperature Superconductors." World Scientific, Singapore, 1992.
9. C. N. R. Rao, *J. Solid State Chem.* **74,** 147 (1986).
10. K. Yvon and M. Francis, *Z. Phys. B. Condens. Matter* **76,** 413 (1989).
11. Y. Tokura, A. Fujimori, H. Matsubara, H. Watabe, H. Takagi, S. Uchida, M. Sakai, H. Ikeda, S. Okuda, and S. Tanaka, *Phys. Rev. B: Condens. Matter* **39,** 9704 (1989).
12. J. E. Greedan, A. H. O'Reilly, and C. V. Stager, *Phys. Rev. B: Condens. Matter* **35,** 8770 (1987).
13. A. Santoro, S. Miraglla, F. Beech, S. A. Sunshine, D. W. Murphy, L. F. Schneemeyer, and J. V. Waszczak, *Mater. Res. Bull.* **22,** 1007 (1987).
14. R. J. Cava, A. W. Hewat, E. A. Hewat, B. Batlogg, M. Marezio, K. M. Rabe, J. J. Krajewski, W. F. Peck Jr., and L. W. Ropp Jr. *Physica C* **165,** 419 (1990).
15. M. H. Whangbo and C. C. Torardi, *Acc. Chem. Res.* **24,** 129 (1991).
16. C. Martin, D. Bourgault M. Hervieu, C. Michel, J. Provost, and B. Raveau, *Mod. Phys. Lett. B* **3,** 993 (1989).
17. R. Vijayaraghavan, C. Michel, A. Maignan, M. Hervieu, C. Martin, B. Raveau, and C. N. R. Rao, *Physica C* **206,** 81 (1993).
18. O. Chmaissem, Q. Huang, E. V. Antipov, S. N. Putilin, M. Marezio, S. M. Loureiro, J. J. Capponi, J. L. Tholence, and A. Santoro, *Physica C* **217,** 265 (1993).
19. T. Siegrist, S. M. Zahurak, D. W. Murphy, and R. S. Roth, *Nature* **334,** 231 (1988).
20. R. J. Cava, T. Siegrist, B. Henssen, J. J. Krajewski, W. F. Peck Jr., B. Batlogg, H. Takagi, J. V. Waszczak, L. F. Schneemeyer, and H. W. Zandbergen, *J. Solid State Chem.* **94,** 170 (1991).